Dust Emission Source Characterization for Visibility Hazard Assessment on Lordsburg Playa in Southwestern New Mexico, USA

Robert Scott Van Pelt (Scott.vanpelt@usda.gov)
USDA-ARS Cropping Systems Research Laboratory https://orcid.org/0000-0002-7036-4032
John Tatarko
USDA-ARS Center for Agricultural Resources Research
Thomas E. Gill
University of Texas at El Paso College of Science
Chunping Chang
Hebei Normal University
Junran Li
University of Tulsa
Iyasu Eibedingil
University of Texas at El Paso College of Science
Marcos Mendez
University of Texas at El Paso College of Science

Research

Keywords: PM10, dust storms, visibility, highway safety, surface emissivity, wind erosion

Posted Date: April 9th, 2020

DOI: https://doi.org/10.21203/rs.3.rs-21670/v1

Version of Record: A version of this preprint was published on December 10th, 2020. See the published version at https://doi.org/10.1186/s40677-020-00171-x.

Abstract

Ephemeral lakes (playas) at the termination of drainages are a common feature of drylands. When dry, playa sediments can be highly wind-erodible, becoming potent local and regional sources of dust and PM 10 , airborne particles with diameters less than 10 μm, causing potentially sudden loss of visibility to travelers on downwind roadways. Lordsburg Playa, in southwestern New Mexico, USA is bisected by Interstate Highway 10. Dust storms emanating from the playa have been responsible for numerous visibility-related road closures (including 39 road closures between 2012- 2019) causing major economic losses, as well as hundreds of dust-related vehicle crashes, causing 41 lost lives in the last 53 years. We investigated the critical wind friction velocity thresholds and the dust emissivities of surfaces representing areas typical of Lordsburg Playa's stream deltas, shorelines, and ephemerally flooded lakebed using a Portable In-Situ Wind ERosion Laboratory (PI-SWERL). Mean threshold friction velocities for PM 10 entrainment ranged from less than 0.30 m s -1 for areas in the delta and shoreline to greater than 0.55 m s -1 for ephemerally flooded areas of the lakebed. Similarly, we quantified mean PM 10 vertical flux rates ranging from less than 500 μ g m -2 s -1 for ephemerally flooded areas of lakebed to nearly 25,000 μg m -2 s -1 for disturbed delta surfaces. The apparently unlimited PM 10 supply of the relatively coarse sediments along the western shoreline however is problematic and indicates that this may be the source area for longer-term visibility limiting dust events and should be a focus area for dust mitigation efforts.

Introduction And Background

Semiarid and arid regions of the world are disproportionate sources of windblown sand (Pye and Tsoar, 2009) and dust aerosols (Prospero et al., 2002; Zobeck and Van Pelt, 2006). Playas (dry or intermittently-wetted lake beds in internal drainage basins), being flat, dry, windswept and unvegetated, are the prominent source areas of dust storms globally (Prospero et al., 2002) including the Chihuahuan Desert of southwest North America (Baddock et al., 2011a, b). One such playa is Lordsburg Playa in Hidalgo County, southwestern New Mexico, USA, just east of the Arizona state line. Lordsburg Playa is not only one of the sources of the most intense dust storms in the Chihuahuan Desert (Rivera Rivera et al., 2010), but is also crossed by Interstate 10 (Figure 1), the southernmost transcontinental highway in the American Interstate Highway System, a major transportation artery extending from Florida to California. Approximately 15,000 vehicles per day, about 30 % of them trucks, crossed the playa in 2016 (Haas, 2017). Lordsburg Playa is the only dust-emitting playa crossed by an interstate highway in Texas or New Mexico. The Union Pacific railroad also crosses the playa parallel to and approximately 30 meters north of the interstate. Plumes of airborne dust and sand crossing the highway close to their source (Figure 2) therefore represent an immediate hazard to roadway traffic due to sudden loss of visibility and resulting driver disorientation (Ashley et al., 2015; Li et al., 2018).

According to the World Health Organization (2018), traffic crashes are the ninth leading cause of death worldwide. In the United States, on average, the annual death toll from motor vehicle crashes due to weather related visibility and vision hazards such as fog, smoke, dust, and blowing sand, exceeds the number of fatalities caused by other weather-related hazards including tornados, floods, tropical cyclones, and lightning (Ashley et al., 2015; Bhattachan et al., 2019).

Windblown (aeolian) dust and sand crossing transportation corridors in drylands is increasingly recognized as a direct threat to human health and safety (Goudie, 2009; Baddock et al., 2013; Middleton, 2017; Li et al., 2017; Zeng-Chao, 2018; Bhattachan et al., 2019; Davari et al., 2019). Dust and sand blowing across roadways causes sudden loss of visibility (Ashley et al., 2015) and reduced traction on the road surface (Davari et al., 2019), and together increase the likelihood for loss of vehicle control and collisions. For example, Goudie (2014) reported that dust-related fatal highway crashes happened in six states in the U.S. in a single year. Numerous case reports have been published of blowing and drifting dust and sand causing highway crashes, especially multi-vehicle incidents on high-speed roads (Pauley, 1996; Laity, 2003; Goudie, 2014; Deetz et al., 2016). The U.S. National Weather Service reported that dust events are the third largest weather-related cause of highway casualties in Arizona, resulting in at least 157 fatalities and 1324 injuries statewide in 50 years (Lader et al., 2016). The authors are not aware of any individual stretch of road in the southwest United States having a greater dust hazard than Interstate 10 across Lordsburg Playa, where more than 40 dust-related traffic fatalities have occurred since 1965, including 21 deaths since 2012; seven persons killed in one dust event in May 2014 and ten killed in 4 dust events during 2017 (Associated Press, 2017; Botkin and Hutchison, 2020).

Dust and sand blowing across highways not only constitutes a direct health and safety hazard, it also causes significant economic impacts. A single traffic fatality is estimated to cost US$1.38 million when medical care, emergency services, productivity over a lifetime, insurance, workplace costs, and legal costs are considered (Blincoe et al., 2010). Beyond healthcare-related costs from crashes, aeolian dust and sand crossing highways disrupts and delays transportation and delivery of goods, services, and people, increases costs for highway maintenance and deployment of public safety personnel, and causes significant property damage; thus, it is a significant "off-site" cost of wind erosion (Pimentel et al., 1995: Baddock et al., 2013). The US Federal Highway Administration (FHWA) (2005) notes that commercial shippers and carriers value transit time at $25 to $200 per hour, depending on the value and perishability of the product being carried, so weather-related delays or detours on major transportation corridors such as caused by dust storms cause significant economic losses as well as health and safety hazards. Only a few studies have provided an in-depth analysis on the occurrence of such events, and little information is available to highway managers on the mitigation and management of this hazard (Li et al, 2018).

At Lordsburg Playa, due to the increasing incidence of crashes, Interstate 10 is now frequently closed to traffic during periods of expected high winds. Such closures result in traffic being diverted onto two-lane secondary highways not designed for heavy truck traffic, representing a detour of 80 km and an hour or more of increased driving times and associated logistical delays, along with damage to these secondary roads. In order to facilitate the detour's increased traffic flow during high wind events and make this route safer, the Arizona Department of Transportation (ADOT) is planning to spend nearly $60,000,000.00 (ADOT, 2019). The New Mexico Department of Transportation (NMDOT) has spent nearly $2,000,000.00 in recent years (Trent Botkin, NMDOT, personal communication) to study and mitigate the dust threat.

Meanwhile other agencies including the U.S. Federal Highway Administration (FHWA), Bureau of Land Management (BLM), USDA Natural Resources Conservation Service (NRCS), and other agencies and contractors have joined with both states' departments of transportation, working diligently together to attempt to mitigate this hazard with engineering-based and biological (vegetation-based) dust control approaches.

Lordsburg Playa comprises several intermittently connected ephemerally flooded dry lakebeds in the northern part of the Animas Basin within the Basin and Range physiographic province and the northwestern Chihuahuan Desert ecoregion. These dry lakebeds represent the bottom of Pleistocene Lake Animas (Allen, 2005). The lakes are the termination of drainage from the Pyramid Mountains, the south and west slopes of Burro Peak, the eastern slopes of the Peloncillo Mountains, and the west and north slopes of the Animas Mountains. The largest and southernmost of the dry lake beds is sometimes named Kathrine Playa, and is the lakebed through which U.S. Interstate 10 traverses. The altitude of the lakebed is approximately 1263 m above mean sea level and the climate is arid with approximately 30 cm of average annual precipitation more than half of which typically falls during the North American Monsoon in July, August and September. Five months of the year have average maximum temperatures in excess of 30^{o} C with June, the hottest month, having an average maximum of 35^{o} C.

Soils in the Lordsburg Playa basin are classified primarily as aridisols of the Hondale series (Fine, mixed, superactive, Thermic Natargid) in the Animas Creek delta and along the western shoreline, Playas series (Fine, mixed, superactive, Sodic Haplocambid) in the ephemerally flooded lakebed, and small areas of vertisols of the Verhalen silty clay loam series (Fine, smectitic, thermic Typic Haplotorrerts) on the eastern shoreline. Although the playa surface is saline and alkaline with occasional salt efflorescences (puffy growths of evaporite minerals on the surface), the surface sediments are comprised of primary silicate and clay minerals with lower concentrations of evaporites (salt minerals) than many other dust-emitting playas in North America (Hibbs et al., 2000; Mitroo et al., 2019).

Vegetation of the area is typical of lower elevation Chihuahuan Desert with dominant shrubs being several species of saltbush (*Atriplex spp.*) and seablight (*Suaeda nigrescens* I.M. Johnst) with alkali sacaton (*Sporobolus airoides* (Torr.) Torr.) as the dominant grass in the saline areas and sand dropseed (*Sporobolus cryptandrus* (Torr.) Gray) and ring muhly (*Muhlenbergia Torreyi* (Kunth) Hitchc.) in well drained sandier areas above the shoreline. Following closure of several mining districts in the Lordsburg basin during the early 20th century, livestock grazing is the primary land use in the surrounding area.

We initiated this study to quantify the dust emissivities of likely potential dust source areas around the Lordsburg Playa. With this knowledge, land managers both public and private in partnership with transportation authorities may be able to prioritize areas for control to mitigate future dust outbreaks, thus protecting human health and safety and reducing economic impacts of blowing dust and sand.

Methods And Materials

We conducted surface dust emissivity testing using a Portable In-Situ Wind ERosion Laboratory (PI-SWERL) (Etyemezian et al., 2007). The PI-SWERL is a computer-controlled aspirated cylindrical chamber approximately 30 cm in diameter that entrains dust by rotating a metallic ring a few centimeters above the soil surface, creating the shear stress necessary to entrain loose particles. The cylindrical chamber is aspirated with 1.67 l s^{-1} of filtered air and a portion of the exhaust is continuously drawn into a DustTrak, a fast response nephelometer (Model 8530, TSI Instruments, Shoreview, Minnesota, USA) to measure PM_{10} (airborne particles with diameter smaller than 10 μm) concentrations. The PI-SWERL has been shown to provide data on dust emissions and surface erodibilities very similar to a larger linear wind tunnel (Sweeney et al., 2008) and has proven useful for estimating dust emissivities at other playas including Yellow Lake, Texas (Sweeney et al., 2016) and the Salton Sea, California (King et al., 2011).

For tests on the Lordsburg Playa surfaces, we set the PI-SWERL on a surface typical of the surrounding area (Figure 3) and initiated a nine-minute (540 s) hybrid test consisting of 60 s of airflow with no movement of the rotating ring, 45 s of accelerating the rotating ring to 2000 rotations per minute (RPM), hold the RPM at 2000 for 60 s, followed by 45 s of rotating ring acceleration to 3000 RPM and 60 s of hold at 3000 RPM, 45 s of rotating ring acceleration to 4000 RPM and 60 s of hold, 45 s of rotating ring acceleration to 5000 RPM and 60 s of hold at 5000 RPM, and finally, 60 s of rotating ring deceleration and continued air flow. Following test initiation, the PI-SWERL was controlled by and all test data, including data from the DustTrak, was logged in an imbedded computer. Test operation data was monitored real-time and the test discontinued to protect the optical bench of the DustTrak if the PM_{10} concentration exceeded 400 mg m^{-3}.

Seven distinct sites in the Lordsburg Playa basin (Figure 1) were tested with the PI-SWERL and at least four replicates were conducted on fresh surfaces at each of the sites. Three of the sites were located on Animas Creek delta deposits on the fringe of the playa south of Interstate 10 and represented land used for cattle grazing designated as sites TS1, TS2, and TS3. Two of the sites had thick, hard, clay-rich lacustrine sediments that dried into indurate crusts of distinct polygons designated sites RFP and NW. Finally, two of the sites were shoreline areas at the eastern and western margins of the lakebed designated as sites EPL and WPL, respectively. At each replicated test location, GPS coordinates were recorded, approximately 100g of the 0 – 5 cm surface sediment was sampled, and the surface threshold friction velocity (u^*_t) was estimated using the airgun and penetrometer technique of Li et al. (2010). Where both undisturbed and disturbed (cattle tracks or vehicle tire tracks) surfaces were sampled for a total of 44 tests, GPS coordinates, and soil samples obtained. Estimates of u^*_t were terminated after 37 tests due to airgun malfunction.

From PI-SWERL data, friction velocities, u* (a measure of shear-related motion in a moving fluids, used to assess potential dispersion of particles in the fluid) were obtained at a frequency of 1 hz by regressing the rotating ring RPM vs Irwin sensor measured friction velocity data provided in the PI-SWERL Operator Manual v1.3 Figure 1.2 (Dust-Quant. Inc., 2011) and entering the instantaneous rotating ring RPM into the resulting regression equation. PI-SWERL estimates of threshold friction velocity u^*_t (the friction velocity at which particles will become entrained in the fluid) were not simple; we almost always saw an initial spike in PM_{10} concentration both when the airflow started during the first few seconds of the test and again at the first few seconds of rotating ring acceleration to 2000 RPM. This spike phenomenon is possibly due to vibration within the PI-SWERL at startup, dislodging particles within the system. Under both these test phases, we saw the PM_{10} concentrations fall to near pre-test levels very soon after the initial spike. We visually determined the $u*_t$ by inspecting the PM_{10} concentration curve to determine when the fresh PM_{10} was being entrained from the ground surface. PM_{10} emissivity expressed as mass per unit time per unit area was calculated by dividing the instrument-determined vertical flux rate data (μg s^{-1}) by the 0.026 m^2 effective area of the rotating ring.

The 2m mean wind velocity that would result in an exceedance of the United States EPA National Ambient Air Quality Standard (NAAQS) for PM_{10} of 150 μg m^{-3} – representing a visibility-reducing dust cloud- was calculated by taking the measured PM_{10} concentration in the PI-SWERL that would result in a 30 m mixed column of air with PM_{10} that would equal or exceed the PM_{10} NAAQS. The value calculated as the trigger concentration for PM_{10} exceedence was 22.5 mg m^{-3}. The friction velocity calculated for this 1 s time step was subsequently entered into Prandtl's equation using 0.4 for von Karman's Constant and a value of 2 X 10^{-5} m for the roughness length to obtain the expected mean windspeed at 2 m at which the PM_{10} NAAQS would be exceeded over similar surfaces. The same calculation based on Prandtl's equation was used to estimate the 2m threshold windspeed for PM_{10} entrainment.

The particle size distribution (PSD) of the surface soil at each site was measured by laser diffraction spectroscopy, generally following the procedures of Sperazza et al. (2004). Soil samples were passed through a 2 mm sieve to remove any gravel or plant debris and 0.2 to 0.6 g of the sieved sample was dispersed in 11.5 ml of a sodium hexametaphosphate solution. The 15 ml tubes containing the dispersed sample were shaken for 8 hours before introduction to the Malvern Mastersizer 2000 (Malvern Instruments, Worcestershire, UK) that had been calibrated using 0.2 g of ISO 12103-1 A4 coarse test dust. For each dispersed sample, three individual PSD determinations were made and the means of each PSD class was calculated. From these means, we determined the percentage of sand ($53 < d < 2000$ μm), silt ($2 < d < 53$ μm), clay ($d < 2$ μm), and PM_{10} ($d < 10$ μm) in each of the soil samples.

Statistical analysis of the data was done using Proc GLM in SAS v9.4. Means were separated using Ryan's Q. Regression relationships between the response parameters and surface factors including soil texture and % PM_{10} was performed in Microsoft Excel graphs by fitting trendlines, linear equations, and R^2 values for the relationships.

Results And Discussion

Mean GPS locations, as well as means and standard deviations of surface sand, silt, clay, and PM_{10} percentages of each site are presented in Table 1. Although some soil PSD variation is evident among the sites, the soil at the west beach site stands out as having much sandier material and much lower content of PM_{10} than any of the others. The western edge of Lordsburg Playa is close to the Peloncillo Mountains and several small drainages empty as alluvial fans directly onto the playa surface from relatively steep terrain. In addition to the nearby steep terrain and resulting coarse sediment transport on the west side of the playa, close examination of aerial photography and satellite images and discussions with local land managers (Trent Botkin, NMDOT, personal communication) has revealed that the dams of several small, decades-old impoundments related to mining and cattle grazing on the mountain slopes have been breached. These impoundments filled with sediment over time and when their dams breached during seasonal rains, huge coarse sediment flows were often formed which in this area have flowed far onto the lakebed surface (Figure 4). Prior systematic analyses of remote sensing imagery have suggested that these zones of contact between coarse sediments and fine playa materials play an enhanced role in initiating dust storms in the Chihuahuan Desert due to the ability of the coarse sandy materials to saltate (hop in the wind) with resultant sandblasting of the finer, wind-entrainable lacustrine sediments (Rivera Rivera et al., 2010).

Test site surface type, disturbance class, as well as friction velocities at threshold ($u*_t$), NAAQS exceedance ($u*_{exc}$), and maximum PM_{10} flux ($u*_{max}$), and the maximum flux rate (MaxQ) and total PM_{10} flux (TotQ) are presented in Table 2.   In general, the sites we tested in the Animas Creek delta (D) and in the beach areas along the shorelines (B) were much more emissive based on MaxQ and TotQ than sites that were ephemerally flooded (L). Sites in the delta to the south, TS1 and TS2, had apparently been cultivated at some time in the past, but all were being used for cattle grazing at the time of the field investigation. At one of the three sites, TS2, furrows had been cut between the natural soil surface to hold water and, hopefully, increase the survival of grass seedlings. The surfaces of these furrow bottoms were very similar to the hard crust polygons found in ephemerally flooded areas and their emission rates were also very similar. For this reason, we considered them to be ephemerally flooded and segregated them from the other tests at this site. In a similar manner, one of the tests at the Road Forks Playa (RFP), an isolated ephemerally flooded area where Interstate 10 enters Lordsburg Playa from the west, was performed on a mantle of aeolian sand that resembled a beach deposit and so we classed that as a beach type surface. With these exceptions, the replicate spots in each site were very uniform in surface characteristics and all PI-SWERL test derived data were used to calculate the means presented in Table 2.

Site characteristics had a significant impact on $u*_t$ ($p<0.0001$), but not $u*_{exc}$ ($p=0.1658$) or $u*_{max}$ ($p=0.7975$). PM_{10} emissions on the other hand were greatly affected by site characteristics with the mean MaxQ of the beach deposits being nearly 2 times that of undisturbed delta soil surfaces whose mean MaxQ was in turn over an order of magnitude greater than the ephemerally flooded lacustrine deposits ($p=0.0018$). Similarly, the TotQ during the test was highly influenced by site characteristics with the mean TotQ of beach deposits being over three times greater than the mean for undisturbed delta soil surfaces which had mean TotQ of more than an order of magnitude greater than the mean for ephemerally flooded lacustrine deposits ($p=0.0003$).

In general, the three sites on the Animas Creek delta, TS1, TS2, and TS3, had soils that were fine textured with shallow surface crusting. At site TS1, the movement of cattle along a fence line had disturbed the surface very close to undisturbed PI-SWERL replicate test spots and we tested them as a subset of the site tests. Similarly, at site TS3, side by side undisturbed and tire-track-disturbed surfaces allowed us to assess the effects of crustal disturbance on PM_{10} emissions and related critical friction velocity parameters. We found no differences in $u*_t$ related to disturbance of the soil crust at either TS1 or TS3 ($p=0.9797$) but the friction velocities at which the NAAQS standard of 150 μg m^{-3} would be exceeded in a 30 m atmospheric column, $u*_{exc}$, was significantly greater for undisturbed soil crusts than for disturbed ($p=0.0305$). The mean values of $u*_{exc}$ for the disturbed spots tested at TS1 and both undisturbed and disturbed spots at TS3, when adjusted to 2m wind speed equivalents, were among very few with less than gale force (<17.5 m s^{-1}) velocities. The undisturbed surface crust at TS3 was very fragile and during a PI-SWERL test of these spots, it was not uncommon to see a very rapid rise in PM_{10} vertical flux rates. Such rapid increases would be consistent with the visual observation at the end of a test where the shear force had displaced a polygon of crust and revealed easily entrainable sediments below, which has been noted as a key process threshold for increasing dust emission at other playas (Cahill et al., 1996). Disturbance also did not significantly influence the friction velocities at which the maximum vertical flux was observed, $u*_{max}$ ($p=0.6491$) although the variances of all friction velocity values were much smaller for the undisturbed sites demonstrating the stabilizing influence of soil crusting.

Although disturbance only influenced one of the $u*_t$ values significantly, it had a very significant effect on the maximum vertical flux of PM_{10} during the testing with disturbed sites having mean emission rates of nearly an order of magnitude greater than undisturbed sites ($p=0.0131$). Similarly, the total PM_{10} emitted by the disturbed sites was more than an order of magnitude greater for the disturbed sites as the undisturbed ($p=0.0266$). These trends of increased PM_{10} emissions with soil crust disturbance are consistent with experimental findings at other wind erodible playa (Cahill et al., 1996; Baddock et al. 2011b) and desert surfaces (Van Pelt et al., 2017; Klose et al., 2019) in the North American drylands, specifically including the effects of cattle activity (Baddock et al., 2011b) and off-highway vehicles (Goossens and Buck, 2009) in increasing dust emission through breakage of surface crusts. The variance among disturbed sites for both these measures was much greater than for undisturbed sites and thus we can state that undisturbed sites were more predictable in their emission rates and total emissions than disturbed sites. This indicates the necessity of limiting disturbance of natural dryland soil crusts in land management plans for mitigating the dust hazard, especially in areas devoid of vegetation where aerodynamic roughness lengths are very small.

Naturally crusted (undisturbed) spots at site TS2 had lower emission rates and totals than the undisturbed spots at TS1 and TS3. However, the ephemerally flooded furrows had emission rates and totals an order of magnitude smaller than the naturally crusted surfaces. These furrows had highly indurate polygonal crusts very similar to the ephemeral lakebeds. Although it was less evident with the disturbed site tests, there is a limitation of PM_{10} supply in the soils of the Animas Creek delta. This is shown in Figure 5 by a drop of emission rate following each local maximum as the RPM and resulting shear force on the surface caused by the PI-SWERL rotating ring was increased and then held steady.

Playa beach deposits at the eastern (EPL) and western (WPL) ends of the pipeline service road that bisects the large playa surface just north of the highway were tested and found to be highly emissive, especially the WPL. The u^*_t means of these sites were not significantly different ($p=0.6630$) and were about the same as those found for undisturbed surfaces in the Animas Creek delta but exhibited greater variance. The mean u^*_{exc} for WPL was significantly lower than that for EPL ($p=0.0112$). In spite of the significantly lower u^*_{exc} for WPL, the mean u*max for WPL, although much more variable, was not significantly lower than the mean for EPL ($p=0.3847$). Although the mean maximum PM_{10} flux rate for WPL was more than twice that for EPL, high variance at both sites precluded any significance in the difference ($p=0.2202$). More dependence on the side of the playa was found for the mean total flux of PM_{10} in which the mean total for WPL is nearly four times that for EPL ($p=0.0589$). The primary test response difference between EPL and WPL was that the tests conducted at WPL did not exhibit any apparent supply limitation (Figure 6) and maintained their emission rates until the RPM and resultant shear stress of the PI-SWERL rotating ring increased to the next level and was held. At EPL, supply limitation was apparent at lower values of friction velocities at the early time steps of the test and only overcame supply limitation at higher friction velocities. Like many of the test surfaces on the Animas Creek delta, the spots tested at WPL also had a mean value of u^*_{exc} that, when converted to 2 m wind speed equivalents, was also less than gale force. Events with 2 m wind speeds in excess of gale force for extended periods of time are rare at inland mountainous locations. Thus, most of the dust entrained will, with the exception of gusts or short periods in which strong pressure gradients are being equilibrated, be entrained with less than gale force velocities.

The two sites tested that represent the ephemerally flooded lakebed included the small Road Forks Playa (RFP) just south of the highway near the western edge of the Lordsburg Playa and a site north of the pipeline access road very near the center of the northern half of the large Kathrine playa (NW). At the RFP test site, four ephemerally flooded surfaces were tested and one that had a mantle of aeolian sand that we classed as a beach type surface. At the NW test site, nine tests were conducted. Values of mean observed u*t were more than 50% greater than for the beach and delta deposits. The tests conducted on the ephemerally flooded surface at RFP did not result in a value of u^*_{exc} that would have exceeded the NAAQS standard for PM_{10}.

At the NW site near the center of the playa, only one of the nine replicate test spots resulted in a NAAQS standard exceedance for PM_{10} in a 30 m column of atmosphere and that value was near the maximum of friction velocities recorded during all phases of testing at all sites. The 2m equivalent wind speed would have exceeded 23 m s^{-1}. The mean value of u^*_{max} for these surfaces was slightly lower than that noted for the other two surface types and had greater variance. The mean maximum vertical flux of PM_{10} from ephemerally flooded surfaces was less than 500 µg m^{-2} s^{-1} and the mean total PM_{10} flux during the nine-minute test was less than 37 mg m^{-2}.

Although the ephemerally flooded lacustrine deposits occupy the predominant surface area in the complex Lordsburg Playa landscape, at least during our March 2018 testing, they exhibited lower PM_{10} emissivities than would be necessary to obscure visibility along the highway unless sand from beach areas or massive coarse sediment flows were advected across large areas of the indurate clay-rich crust or the crust was disturbed by activities such as off-road vehicle traffic or cattle grazing. The trampling of crusts by the movement of cattle was demonstrated to increase dust emissions during controlled wind tunnel tests on another playa in southern New Mexico (Baddock et al., 2011b) and it would likely do so at Lordsburg Playa. The playa has been closed by the United States Bureau of Land Management to off-highway vehicle use since 1998 'to reduce impacts to the soil on the Lordsburg Playa. Once the soil surface is disturbed, it is highly susceptible to wind erosion' (United States Department of the Interior, 1998); however, observations of the authors and New Mexico state employees suggest that crust crushing off-rod recreational vehicle use still takes place on the playa surface. Rigorous monitoring and enforcement of this prohibition should be increased, since even a small area of disturbed playa in the wrong place and an unfortunate squall of wind could initiate a dust plume crossing the highway and dangerously reducing visibility.

Conclusions

Lordsburg Playa in New Mexico, USA is representative of playa (dry lakebed) environments in desert regions where windblown dust emissions create traffic safety and crash hazards, and a priority site for environmental remediation to improve highway safety and reduce detour-related delays and losses. We tested the surface emissivity characteristics at sites representing different landscape positions, management histories, and surface crust disturbance at Lordsburg Playa using a PI-SWERL. A wide range of values for threshold friction velocity, friction velocity at which the National Ambient Air Quality Standard would be exceeded in a 30 m column of air (representing formation of a dust cloud), PM_{10} (fine dust) vertical flux rates, and total PM_{10} vertical flux during the nine minute test are indicative of the complexity of the surfaces encountered in the immediate vicinity of Lordsburg Playa. We also found that the critical friction velocities and emissivities were not strongly dependent on the surface sediment texture but were highly dependent on surface crust strength, thickness, and disturbance.

From our data, we conclude that the actual lake bed surface is not strongly dust-emissive when intact even when dry, but the shoreline margins or beach areas and areas of the Animas Creek delta are highly dust-emissive and should be the focus areas of management to mitigate wind erodibility including limiting disturbance and augmenting native sediment trapping vegetation when possible. The western shoreline of the playa is the most emissive of the sites tested and is one of the few areas without dust supply limitation even though the surface sediments contain by far the lowest percentage of PM_{10}; this is likely due in part to legacy sediment control structures (dams and berms) on the slopes above the playa which are failing and releasing pulses of debris onto the western playa surface. For these reasons, this area should be a priority for dust emission control measures followed by areas on the Animas Creek delta that develop more fragile crusts. In order to improve highway safety and reduce the risk of continued visibility-related crashes and shutdowns, the playa should be carefully monitored for and protected against activities that disturb the crust and increase dust emissions.

List Of Abbreviations

ADOT – Arizona Department of Transportation

B – Beach deposit, usually sandy material above the playa flood pool

BLM – U.S. Department of the Interior Bureau of Land Management

D – Delta deposits from Animas Creek, mostly south of Interstate 10

EPL – PI-SWERL test site at the east end of Pipeline Road (a beach deposit)

GPS – Global Positioning System

L – Lacustrine deposits in ephemerally flooded areas of the playa, usually clay-rich and highly indurated

MaxQ – The greatest 1 second vertical flux of PM_{10} during a PI-SWERL test, an index of surface emissivity

NAAQS – U.S. Environmental Protection Agency National Ambient Air Quality Standards

NMDOT – New Mexico Department of Transportation

NRCS – U.S. Department of Agriculture Natural Resources Conservation Service

NW – PI-SWERL test site in the center of the ephemerally flooded playa

PI-SWERL – Portable In-Situ Wind ERosion Laboratory

PM_{10} – Particles with diameters less than ten micrometers

PSD – Particle Size Distribution

RFP – PI-SWERL test site at the Road Forks Playa, an ephemerally flooded surface south of Interstate 10

SAS – Statistical Analysis Software published by the SAS Institute

TotQ – The total PM10 vertical flux produced during the 540 second PI-SWERL test

TS1 – PI-SWERL test Site 1 on the Animas Creek Delta

TS2 – PI-SWERL test Site 3 on the Animas Creek Delta

TS3 – PI-SWERL test Site 3 on the Animas Creek Delta

u^* - Friction velocity

u^*_{exc} – Friction velocity at which sufficient PM_{10} vertical flux was measured to exceed NAAQS

u^*_{max} – Friction velocity at which the greatest vertical flux of PM_{10} was measured

u^*_t – Threshold friction velocity, the friction velocity at which vertical flux of PM10 was initiated

WPL – PI-SWERL test site at the west end of Pipeline Road (a beach deposit)

Declarations

Availability of Data – The authors will provide the data upon request

Conflicts and Competing Interests – The authors have no conflict of interest or completing interest with any entity responsible for management of the Lordsburg Playa

Funding - Support is acknowledged for various parts of this work from grants NNX16AH13G and 80NSSC19K0195 from NASA and Project UTEP-01-13 from the Center for Advancing Research in Transportation Emissions, Energy, and Health (CARTEEH), a U.S. Department of Transportation University Transportation Center.

Authors' Contributions – RSVP and TEG conceived the investigation; TEG provided funding of UTEP personnel; JT and JL provided equipment; RSVP, JT, CC, IE, and MM performed field investigations; RSVP and JT curated the data, RSVP analyzed the data; IE analyzed the PSD of surface sediments and provided images used for figures 1 – 4; RSVP wrote the original draft; all authors reviewed and edited the manuscript in its current form.

Disclaimers

Mention of trade names is for informational purposes only and does not infer endorsement by nor exclusion of other similar products by the United States Department of Agriculture or other agencies supporting this work.

The United States Department of Agriculture is an equal opportunity employer and provider.

References

ADOT (Arizona Department of Transportation) (2019) U.S. 70, Safford to New Mexico State Line Interstate Detour Needs Study. Report Prepared for the Arizona Department of Transportation, December, 2019. 69 pp.

Allen BD (2005) Ice age lakes in New Mexico. *In:* Lucas SG, Morgan GS, and Zeigler KE (Eds) New Mexico's Ice Ages. NM Mus Nat Hist Sci Bull No 28. 8 pp.

Ashley WS, Strader S, Dziubla CC, and Haberlie A (2015) Driving blind: Weather-related vision hazards and fatal motor vehicle crashes. Bull Am Meteorol Soc 96:755-778.

Associated Press (2017) 2 killed in freeway crash in NM dust storm. http://www.lcsun-news.com/story/news/local/2017/02/24/2-killed-freeway-crash-nm-dust-storm/98369206/

Baddock MC, Gill TE, Bullard JE, Dominguez-Acosta M, and Rivera-Rivera N (2011a) Geomorphology of the Chihuahuan Desert based on potential dust emissions. J Maps 7:249-259.

Baddock MC, Zobeck TM, Van Pelt RS, and Fredrickson EL (2011b) Dust emissions from undisturbed and disturbed, crusted playa surfaces: Cattle trampling effects. Aeolian Res 3:31-41.

Baddock MC, Strong CL, Murray PS, and McTainsh GH (2013) Aeolian dust as a transport hazard. Atmos Environ 71:7-14.

Bhattachan A, Okin GS, Zhang J, Vimal S, and Lettenmaier DP (2019) Characterizing the role of wind and dust in traffic accidents in California. GeoHealth 3(10):307-328.

Blincoe L J, Miller T R, Zaloshnja E, and Lawrence BA (2015) The economic and societal impact of motor vehicle crashes, 2010. Washington, DC: National Highway Traffic Safety Administration Report DOT HS 812 013.

Botkin T, and Hutchinson B (2020) Lordsburg Playa Dust Storm Mitigation Update. Presentation at the USA National Weather Service 9th Dust Storm Workshop, March 2020, Coolidge, Arizona, online at https://www.weather.gov/media/psr/Dust/2020/9_BOTKIN_DustMitigation_AZ_2020.pdf

Cahill TA, Gill TE, Reid JS, Gearhart EA, and Gillette DA (1996) Saltating particles, playa crusts, and dust aerosols at Owens (dry) Lake, California. Earth Surf Proc Landforms 21:621-639.

Davari M, Khabiri MM, and Tafti M (2019) The Effect of Pollutants, Dust and Dune Sand Covered Over the Surface of Asphalt Pavements on Road Safety (Case Study, Sistan and Blouchestan Province, Iran). Environmental Studies 4:1123 - 1129. (in Persian, English abstract)

Deetz K, Klose M, Kirchnerand I, and Cubasch U (2016) Numerical simulation of a dust event in northeastern Germany with a new dust emission scheme in COSMO-ART. Atmos Environ 126:87–97.

Etyemezian V, Nikolich G, Ahonen S, Pitchford M, Sweeney M, Purcell R, Gillies J, and Kuhns H (2007) The Portable In-Situ Wind ERosion Laboratory (PI-SWERL): a new method to measure PM_{10} potential for windblown dust properties and emissions. Atmos Environ 41:3789-3796.

Federal Highway Administration (FHWA) (2005) Measuring Travel Time in Freight-Significant Corridors. US Department of Transportation, Federal Highway Administration, Office of Freight Management and Operations.

Goossens D, and Buck B (2009) Dust emission by off-road driving: Experiments on 17 arid soil types, Nevada, USA. Geomorphology 107: 118-138.

Goudie AS (2014) Desert dust and human health disorders. Environ Intl 63:101-113.

Haas TP (2017) Traffic Counts New Mexico Interstates. Report prepared by the New Mexico Department of Transportation for the Transportation Infrastructure Revenue Subcommittee Meeting October 10, 2017.

Hibbs B, Lee M., Hawley JW, and Kennedy JF (2000) Some notes on the hydrogeology and groundwater quality of the Animas Basin system, southwestern New Mexico. New Mexico Geol Soc Fall Field Conf Guidebook 51:227-234.

King J, Etyemezian V, Sweeney M, Buck BJ, and Nikolich G (2011) Dust emission variability at the Salton Sea, California, USA. Aeolian Res 3:67-79.

Klose M, Gill TE, Etyemezian V, Nikolich G, Zadeh ZG, Webb NP, and Van Pelt RS (2019) Dust emission from crusted surfaces: Insights from field measurements and modelling. Aeolian Res 40:1-14.

Lader G, Raman A, Davis JT, and Waters K (2016) Blowing dust and dust storms: One of Arizona's most underrated weather hazards. NOAA Tech Memor NWS-WR-290.

Laity J (2003) Aeolian destabilization along the Mojave River, Mojave Desert, California: linkages among fluvial, groundwater and aeolian systems. Phys Geogr 24:, 196–221.

Li J, Okin GS, Herrrick JE, Belnap J, Munson SM, and Miller ME (2010) A simple method to estimate threshold friction velocity of wind erosion in the field. Geophys Res Letters 37:L10402, doi:10.1029/2010GL043245.

Li J, Kandakji T, Lee JA, Tatarko J, Blackwell J, Gill TE, and Collins JD (2017) Blowing dust and highway safety in the southwestern United States: Characteristics of dust emission "hotspots" and management implications. Sci Tot Environ 621:1023-1032, doi:10.1016/j.scitotenv.2017.10.124.

Middleton NJ (2017) Desert dust hazards: A global review. Aeolian Res 24:53-63.

Mitroo D, Gill TE, Pratt KA, and Gaston CJ (2019) $ClNO_2$ production from N_2O_5 uptake on saline dusts: New insights into potential inland sources of $ClNO_2$. Environ Sci Tech 53:7442-7452.

Pauley PM, Baker NL, Barker EH (1996) An observational study of the "Interstate 5" dust storm case. Bull Am Meteorol Soc 77: 693–720.

Pimentel D, Harvey C, Resosudarmo P, Sinclair K, Kurz D, McNair M, Crist S, Shpritz L, Fitton L, Saffouri R, and Blair R (1995) Environmental and economic costs of soil erosion and conservation benefits. Science 267:1117–1123.

Prospero JM, Ginoux P, Torres O, Nicholson SE, and Gill TE (2002) Environmental characterization of global sources of atmospheric dust identified with the Nimbus-7 Total Ozone Mapping Spectrometer (TOMS) absorbing aerosol projects. Rev Geophys 40(1): 1002, doi:10.1029/2000RG000095.

Pye K, and Tsoar H (2009) Aeolian Sand and Sand Dunes. Springer, Berlin, 476 pp.

Rivera-Rivera NI, Gill TE, Bleiweiss MP, and Hand JL (2010) Source characteristics of hazardous Chihuahuan Desert dust outbreaks. Atmos Environ 44:2457-2468.

Sperazza M, Moore JN, and Hendrix MS (2004) High resolution particle size analysis of naturally occurring very fine-grained sediment through laser diffractometry. J Sedimentary Res 74:736-743.

Sweeney MR, Zlotnik VA., Joeckel RM, and Stout JE (2016) Geomorphic and hydrologic controls of dust emissions during drought from Yellow Lake playa, West Texas, USA. J Arid Environ 133:37-46.

Sweeney M, Etyemezian V, Macpherson T, Nickling W, Gillies J, Nikolich G, and McDonald E (2008) Comparison of PI-SWERL with dust emission measurements from straight-line wind tunnel. J Geophys Res 113, F01012, doi:10.1029/2007JF000830.

United States Department of the Interior, Bureau of Land Management (1998) Emergency Closure of the Lordsburg Playa to Off-HIGHWAY VEHICLES (OHV), Hidalgo County, NM. Federal Register 63(122):34661.

Van Pelt RS, Baddock MC, Zobeck TM, D’Odorico P, Ravi S, and Bhattachan A (2017) Total vertical sediment flux and PM_{10} emissions from disturbed Chihuahuan Desert surfaces. Geoderma 293:19-25.

World Health Organization (2018) Global status report on road safety 2018. World Health Organization, Geneva.

Zheng-chao HU (2018) The Wind-blown Sand Hazard Potential Evaluation of Highway on Dry up Lake-basin Region of Taitema Lake. Territory & Nat Res Study 2: 13.

Zobeck TM, and Van Pelt RS (2006) Wind-induced dust generation and transport mechanics on a bare agricultural field. J Hazard Mater 132:26-38.

Tables

Table 1. Mean and standard deviation of longitude, latitude, percent sand, silt, clay and PM_{10} for the surface sediment samples at the test sites.

Site (Surface Class)*		Longitude Degrees W	Latitude Degrees N	Sand %	Silt %	Clay %	PM_{10} %
TS1 (D)	Mean	108.854	32.255	17.79	69.2	12.29	41.30
	St. Dev.	1.91 E-5	8.64 E-5	1.01	1.10	0.50	1.36
TS2 (D)	Mean	108.868	32.254	28.64	57.42	13.94	42.25
	St. Dev.	3.86 E-5	3.47 E-5	4.94	4.16	3.16	7.40
TS2 (L)	Mean	108.868	32.254	30.66	57.16	12.18	37.57
	St. Dev.	1.04 E-4	3.98 E-5	5.37	7.05	1.67	2.62
TS3 (D)	Mean	108.878	32.267	18.01	70.10	11.90	45.24
	St. Dev.	8.03 E-5	5.4 E-5	1.08	1.29	1.32	3.41
RFP (L)	Mean	108.943	32.242	29.02	62.27	8.70	33.72
	St. Dev.	5.89 E-4	6.68 E-4	12.27	12.00	0.51	2.93
RFP (B)	Mean	108.944	32.242	56.72	36.17	7.11	25.22
	St. Dev.	--	--	--	--	--	--
NW (L)	Mean	108.908	32.322	17.52	54.62	27.85	57.73
	St. Dev.	3.18 E-4	2.47 E-4	3.88	1.95	2.81	4.55
EPL (B)	Mean	108.832	32.333	41.33	45.35	13.32	42.55
	St. Dev.	1.65 E-4	7.11 E-5	7.13	6.13	1.70	7.06
WPL (B)	Mean	108.933	32.315	84.59	12.23	3.17	10.80
	St. Dev	1.93 E-5	4.41 E-5	13.00	10.76	2.24	8.83

*surface classes are D = Delta, L = Lake, and B = Beach

Table 2. Surface class (Delta, Lake, or Beach), disturbance class (Undisturbed or Disturbed), and mean and standard deviation of threshold friction velocity ($u*_t$), friction velocity at which the NAAQS standard would be exceeded in a 30 m tall column of air ($u*_{exc}$), friction velocity at which the maximum rate of PM_{10} vertical flux is observed ($u*_{maxQ}$), the maximum rate of PM10 vertical flux observed (Max Q), and the total PM_{10} vertical flux for the nine minute PI-SWERL test (Tot Q) of each sample site.

Site	Surf. Class	Disturb. Class		u^*_t (m s^{-1})	u^*_{exc} (m s^{-1})	u^*_{maxQ} (m s^{-1})	Max Q (µg m^{-2} s^{-1})	Tot Q (µg m^{-2})
TS1	D	U	Mean	0.31	0.80	0.81	1325.48	84217
			St. Dev.	0.02	0.02	0.00	919.87	69106
TS1	D	D	Mean	0.31	0.62	0.81	11030.94	845554
			St. Dev.	0.02	0.07	0.01	5498.17	5168485
TS2	D	U	Mean	0.26	0.74	0.80	3098.75	193221
			St. Dev.	0.05	0.12	0.02	2021.42	131854
TS2	L	U	Mean	0.31	--	0.80	223.60	16733
			St. Dev.	0.01	--	0.00	36.49	2287
TS3	D	U	Mean	0.24	0.60	0.80	1248.26	999201
			St. Dev.	0.05	0.15	0.02	8697.52	832504
TS3	D	D	Mean	0.31	0.50	0.68	24977.63	2226249
			St. Dev.	0.02	0.03	0.05	1778.07	682823
RFP	L	U	Mean	0.36	--	0.81	476.06	45648
			St. Dev.	0.06	--	0.00	406.79	77958
RFP	B	U	Mean	0.39	0.77	0.81	2450.36	288993
			St. Dev.	--	--	--	--	--
NW	L	U	Mean	0.56	0.81	0.80	561.84	36857
			St. Dev.	0.10	--	0.02	717.75	49034
EPL	B	U	Mean	0.30	0.72	0.81	7561.78	788012
			St. Dev.	0.10	0.08	0.00	12282.01	1266773
WPL	B	U	Mean	0.28	0.50	0.80	17182.49	2727300
			St. Dev.	0.04	0.05	0.02	6844.97	1084141

Figures

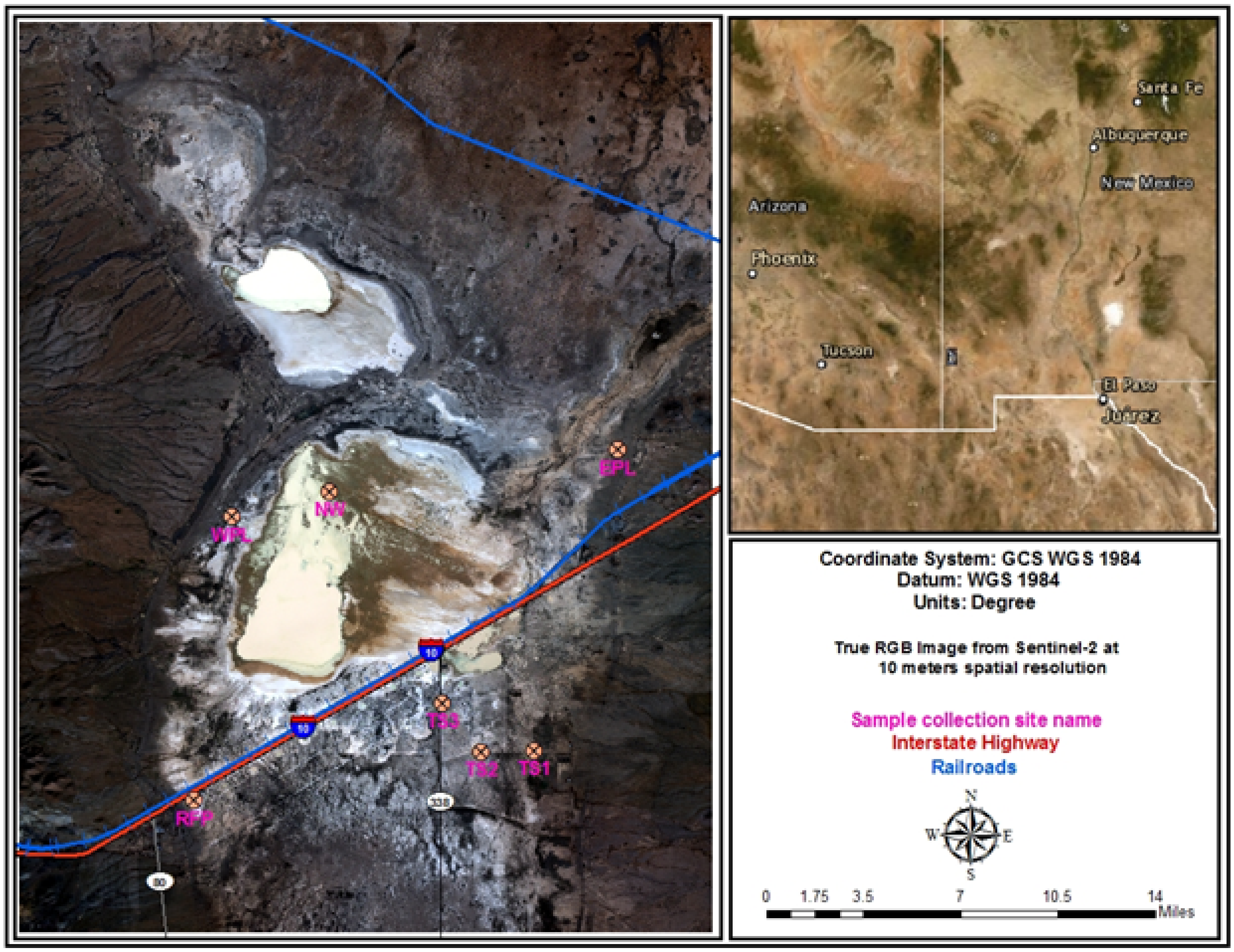

Figure 1

Aerial image of Lordsburg Playa dissected by Interstate 10 showing the locations (crossed circles) of surfaces that were tested with the PI-SWERL as listed in Table 1.

Figure 2

Dust clouds blowing across Interstate Highway 10 on Lordsburg Playa while the highway is open to automobile and truck traffic, March 22, 2016.

Figure 3

PI-SWERL in test configuration on an undisturbed surface at the eastern beach area (EPL).

Figure 4

Aerial photograph of area on the west of Lordsburg Playa showing erosional head cutting in the left portions of the picture and subsequent deposition of eroded sediment on the playa surface in the right-hand portions of the image.

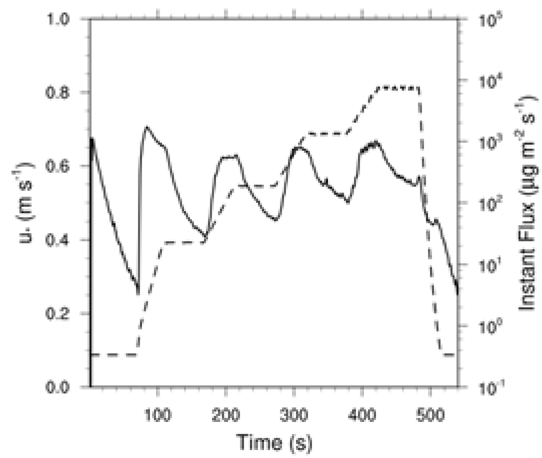

Figure 5

PI-SWERL test response curve showing PM10 supply limitations. The dashed line represents the friction velocity (u*) and the solid line is the instantaneous vertical flux of PM10. This test was from an area that is ephemerally flooded (L).

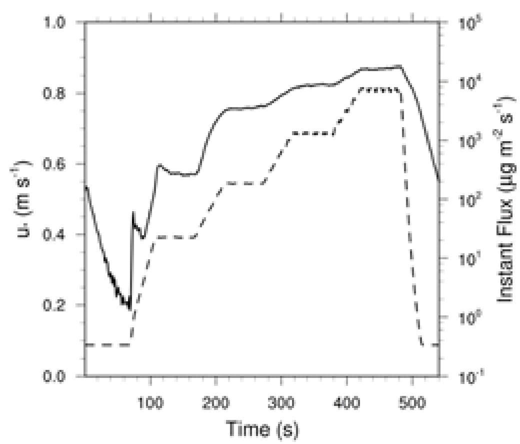

Figure 6

PI-SWERL test response curve showing no PM10 supply limitations once threshold friction velocity (u*t) has been exceeded. The dashed line represents the friction velocity (u*) and the solid line is the instantaneous vertical flux of PM10. This test was from the western beach area (WPL).